NUMERICAL SIMULATION OF ORGANISED AND SELF-ORGANISED SEPARATED FLOWS IN THE FRAMEWORK OF MULTIBLOCK COMPUTATIONAL TECHNOLOGIES

S.A. Isaev

Academy of Civil Aviation,
196210 Sankt-Petersburg, Russia

Introduction

The vortex intensification mechanism of heat transfer on the dimpled surfaces and crossed flow control of the bodies with additional construction elements like forward disks and vortex cells is analyzed by numerical methods. Self-organizing 3D vortex structures generating within dimple enhance the heat transfer from the wall [1], and the effect on the boundary layer by bleeding-suction or rotating central body of the vortex cell results in diminishing of the separation effect influence accompanied by the reduction of the body drag and increasing of lift force [2]. 3D vortex like toroid generated in the gap between forward disk and leading body edge is responsible for the pressure deficit at this region and, as a sequence, additional thrust that almost compensates the forward disk drag [3]. Vortex strain at the forward separation region at the angle of attack different from zero causes the effect of head stability for the cylinder with forward disc [4].

Numerical technology

The known mathematical model based on the system of the Reynolds equations written for Courtesan velocity components for incompressible viscous fluid is used to describe the separation flow. Low – Reynolds number $k - \omega$ Menter's model is used for describing the turbulent effects [5]. For the calculation of the governing equations implicit factorised algorithm based on the procedure SIMPLEC to correct pressure block is used. Numerical calculations of different flow types are carried out using the crossing grids of different scales. This technique allows to simulate 3D and multiconnected regions by crossing grids of simple topology.

Calculating algorithm has been tested considering the low velocity flow in the flat channel with circular vortex cell. Numerical data were compared with experimental one obtained in IM MGU [7].
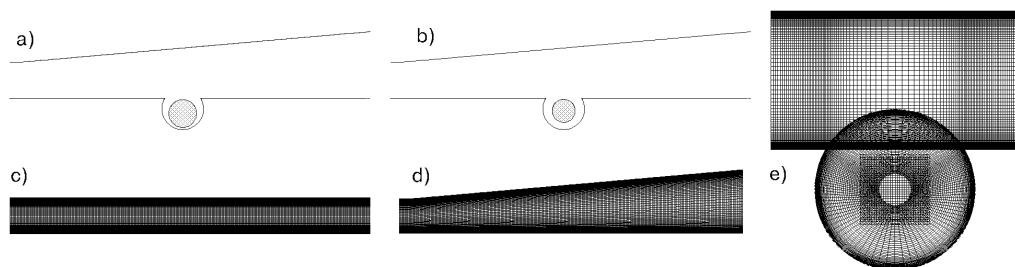

Fig. 1. The schemes of the diffuser channel with vortex cells including central rotating body.
a) base variant; b) modified variant; c) calculating grid of flat channel; d) calculating grid of diffuser channel; e) a piece of the multiblock grid of flat channel at the circular vortex cell.

Report Documentation Page

Report Date 23 Aug 2002	Report Type N/A	Dates Covered (from... to) -

Title and Subtitle Numerical Simulation of Organised and Self-Organised Separated Flows in the Framework f Multiblock Computational Technologies	**Contract Number**
	Grant Number
	Program Element Number
Author(s)	**Project Number**
	Task Number
	Work Unit Number
Performing Organization Name(s) and Address(es) Institute of Theoretical and Applied Mechanics Institutskaya 4/1 Novosibirsk 530090 Russia	**Performing Organization Report Number**
Sponsoring/Monitoring Agency Name(s) and Address(es) EOARD PSC 802 Box 14 FPO 09499-0014	**Sponsor/Monitor's Acronym(s)**
	Sponsor/Monitor's Report Number(s)

Distribution/Availability Statement Approved for public release, distribution unlimited

Supplementary Notes See also ADM001433, Conference held International Conference on Methods of Aerophysical Research (11th) Held in Novosibirsk, Russia on 1-7 Jul 2002

Abstract

Subject Terms

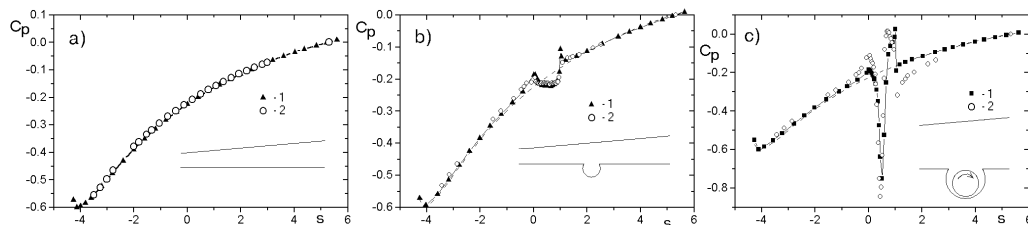| **Report Classification** unclassified	**Classification of this page** unclassified
Classification of Abstract unclassified	**Limitation of Abstract** UU

Number of Pages 6

Fig. 2. Distribution of the pressure coefficient along the symmetry line of the low side of the diffuser channel.
a) without the vortex cell; b) passive vortex cell at Re = 1.35·10⁵; c) base variant, active vortex cell at Re = 6·10⁴; 1– numerical data; 2 – experimental data. The dotted line describes the pressure distribution in the diffuser channel without vortex cell.

Calculating grids using for methodology investigation of the separation flow in the diffuser channel with passive and active vortex cell including the rotating body are presented in Fig.1 The correlation of numerical and experimental distributions of pressure coefficient in the channel without vortex cell, and when there is passive or active vortex cell (the tangential velocity on the body surface is 1,7) justifies reliability of the developed method.

Results

Numerical results of the turbulent flow that crosses the circular cylinder with vortex cell which has round edges and separating plate in the wake are presented in Fig.3. The radii of the edges are different. The back edge has bigger radius.

Turbulent subcritical regime is calculated in the frame of steady model at Re = 1.45·10⁴. The variations of the aerodynamics characteristics of the cylinder with growing suction velocity on the surface of the central body of the cell has abrupt behavior. There is a threshold value of U_n that is equal approximitly to 0,03 at which calculated cylinder drag is reduced in 4 times. The same result has been observed for cylinder with elliptic vortex cells [8]. The reason of the behavior of C_x is transformation of the flow over the cylinder: abrupt removal of the separation point to the back flow stagnation point is accompanied with shortening of circulation region of near wake. Increasing of the radius of back cell edge enhances cell influence on the flow. The
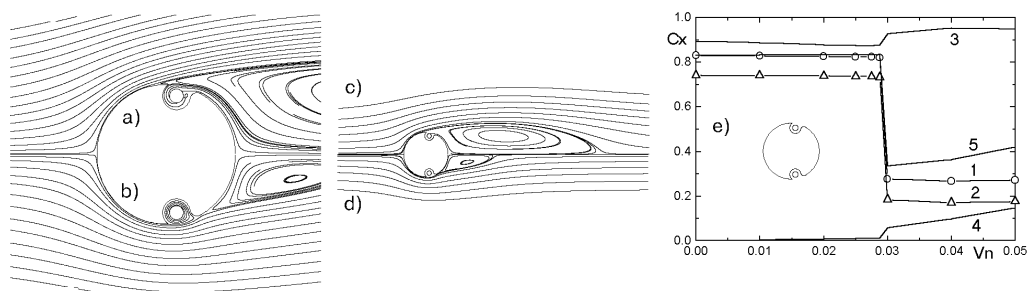

Fig. 3. Flow structure behind the cylinder with vortex cell at subcritical regime and at different suction velocity:
a, c) U_n= 0.0289; b, d) U_n = 0.03; e) variation of cylinder drag and its components with suction velocity U_n: 1 – cylinder drag; 2 –profile drag; 3 – skin friction (multiplied in 10 times); 4 – additional drag coefficient estimated on power suction; 5 – total drag coefficient (it takes into account the waste energy).
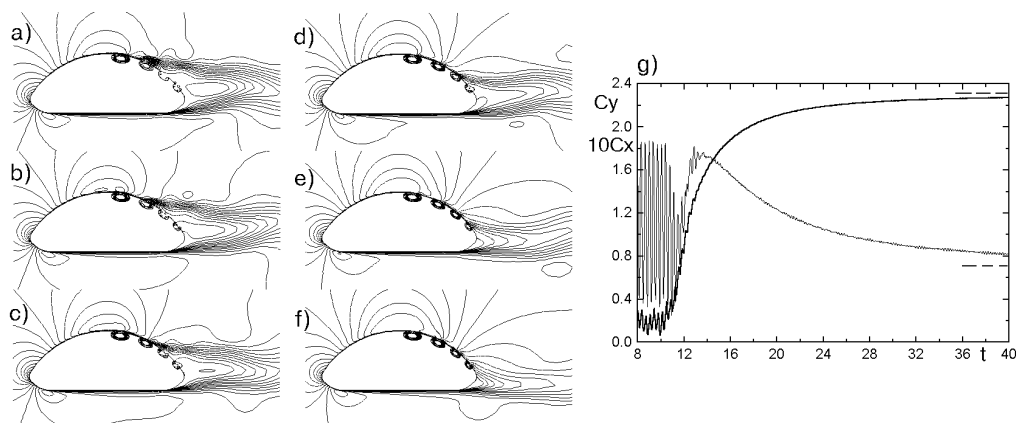
Fig. 4. Evolution of isotahs of longitudinal velocity component for transition regime.
a) t = 10.4; б) 10.8; в) 11.2; г) 11.6; д) 12.0; е) 12.4; g) the variations of C_x and C_y with time for starting moment of the stabilization regime. The dotted line shows the characteristics of steady regime.

cylinder drag reduction tends to be stronger. The edge radius of 0,05 results in total drag reduction about 10% in comparison with the case when the cell edge is sharp and approximately in 2 times in comparison with the drag of smooth cylinder.

The developed multiblock algorithm is used further to study unsteady separation flow behind the thick profile with active vortex cells (VC). The order of the principal steps in the motion of profile with VC is following: the unsteady flow regime is calculated for 10 units of dimensionless time for the body with passive vortex cells from the moment of contact of fluid and body.

Time interval is assigned 0.01. The Peire's scheme of second order approximation is used. Further (in interval 10-11 units) the velocity suction in VC is increased from 0 to 0.05 (basic variant for steady regime) and is kept constant up to development of steady flow crossed cylinder.

The transition from self-oscillating phase to steady flow crossed body is the most interesting. It begins when the circulation in the vortex cell starts (t=10) and continues to the end of visible oscillations of the near wake (t~13, Fig. 4). Suction in VC intensifies flow circulation inside it and changes essentially flow structure over the cylinder. Naturally, there is time delay between the moment of suction velocity increasing and variations of coefficients C_x and C_y. However, beginning from the time t = 11.5, operating effect is already prominent. The growth of lift force, that is quite expected, accompanies by the increasing of the cylinder drag that reaches its maxim value at self-oscillating regime. Last phase of flow over the thick profile with active vortex cells is characterized by the flow stabilization when integral characteristics are approaching to their asymptotic values.

Numerical visualization of laminar flow over the complex construction combining small forward disc and cylinder at middle angle of attack is presented in Figs. 5 and 6. For comparison, the visualization of the same construction when angle of attack is nearly zero and equal to 6o is also presented.
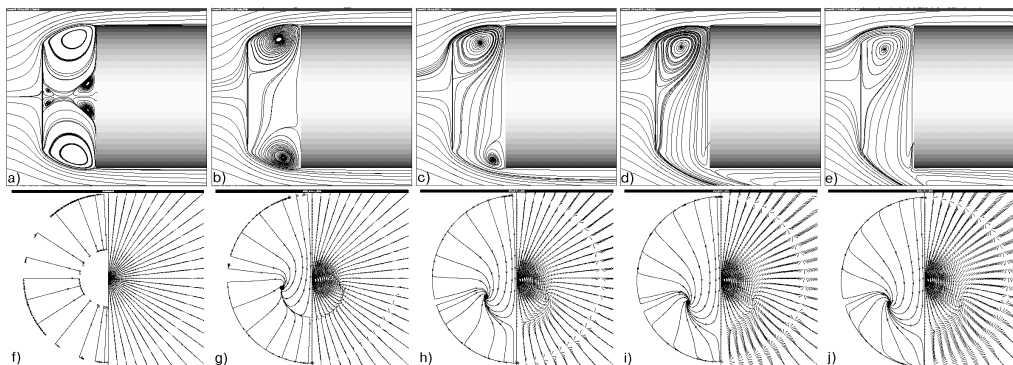
Fig. 5. Laminar flow (Re=500) along the cylinder with forward disk ($R = 0.75$; $l = 0.375$ of cylinder diameter) at different angles of attack α in longitudinal (a,b,c,d,e) and face (f, g, h, i, j) planes. a, f – α=0°; b, g – 0.5^o; c, h – 2°; d, i – 5°; e, j – 8°.
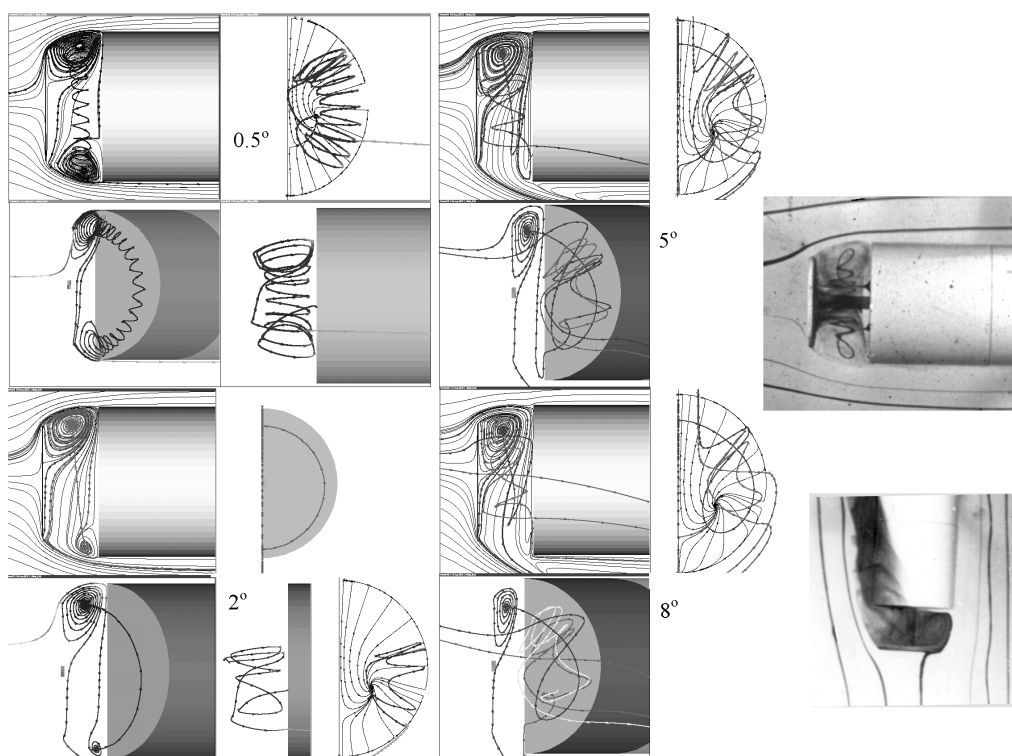

Fig . 6. Visualization of the vortex flow in the forward separation region of complex construction (dick-cylinder) at different angles of attack of laminar oncoming flow.

105

At the angles of attack different from zero there are mainly the transformation of 3D separation flow in the gap between disk and cylinder face and a little strain of toroid vortex. It is important that the transition to the complex vortex structure occurs abruptly and later on it changes not very mush with increasing of angle of attack in considered interval. The distinctive characteristics of the flow are typical for the tree-dimensional separation flows. The specific points like focus on the cylinder face (Fig.5) are mass sources that initiate swirl tornado-like flows clearly observed on the visualized pictures of flow in water channel (Fig.6). The disposition of these specific points is not change practically with growth of angle from 0 to 8°.

The fluid flow like the flow in vortex tube appears in the separation region occupied the space between disk and cylinder face. The opposite swirling flows along the center core from down wind side to the up wind side and along the periphery from upwind to downwind side are taken place. The spatial separation region becomes unclosed. The fluid comes inside it and ejects to side surface of the cylinder as two swirl jets. These flow structure elements are responsible for the effect of head stability [9].
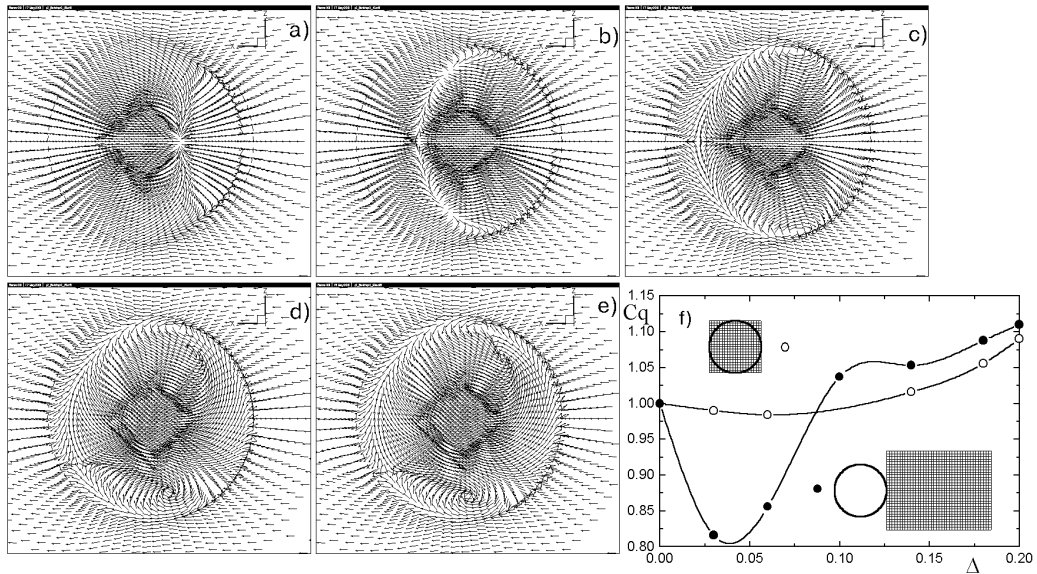

Fig. 7. The evolution of the vector velocity direction inside boundary layer within spherical dimple with growth of its relative depth Δ in turbulent flow (Re=2.3·10^4).
a – Δ=0.06; b – 0.1; c – 0.14; d – 0.18; e – 0.2; f) dependence of the relative heat transfer Cq with Δ for the area covering the dimple and the surface behind it

The analysis of turbulent flow over spherical dimple (Fig.7) supports the above-mentioned observations concerning spatial separation flows. The increasing of the dimple depth enlarges spreading of the separation flows and their strength. When the parameter $\Delta = 0.14$ grows to $\Delta = 0.18$, the vortex structure within dimple changes sharply. Two-cells vortex structure is transformed to mono vortex like tornado. This transformation causes the heat transfer growth within dimple and behind it in the same rate. The dimple diameter is choused as normalize factor.
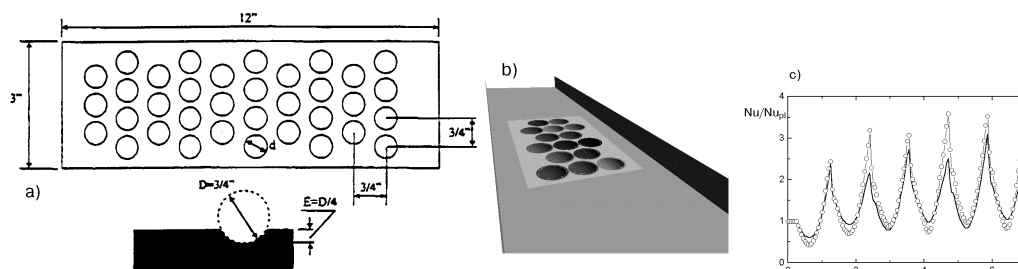
Fig. 8. The wall configurations with dimple array in experimental (a) and numerical (b) investigations. c) the variation of relative heat transfer with number of dimples for the dimple strip width of 4.266 and 2.133.

The effect of vortex heat transfer enhancement is analyzed for the dimple array of big depth (0.28) and density (the step between dimple center is 1.155). This dimple array is placed on the side of flat narrow channel (Fig. 8). The calculated value of C_q is an order 2.4 for the internal dimple row, i.e., the same as in experiments with the great number of dimples [10]. The pressure drop in the channel changes very small in comparison with the prop in the smooth flat channel.

So, for the different type of separation flows (with fixed and removal separation point, bounded by walls and in free flows) the typical flow-generated structure elements that responsible for the aeromechanics and thermophysics effects are determined.

REFERENCES

1. **Isaev S.A., Leontiev A.I., Usachov A.E.** Numerical study of the eddy mechanism of enhancement of heat and mass transfer near a surface with a cavity // J. Engineering Physics and Thermophysics. 1998. Vol.71. No.3. P.481-487.
2. **Baranov P.A., Isaev S.A., Prigorodov Yu.S., Sudakov A.G.** Numerical simulation of laminar flow round a cylinder with passive and active vortex cells // Technical Phys. Lett. 1998. Vol.24. No.4. P.301-304.
3. **Isaev S.A.** Numerical simulation of the axisymmetric low-velocity flow around a cylinder with coaxial disks // J. Eng. and Termophys. 1995. Vol.68. No.1. P.16-21.
4. **Guvernyuk S.V., Isaev S.A., Sudakov A.G.** Identification of the bow stabilization mechanism by numerical simulation of the laminar asymmetric flow of a viscous incompressible fluid past a cylinder with a projecting disk // Technical Phys. 1998.Vol.43. No.11. P.1397-1400.
5. **Menter F.R.** Two-equation eddy-viscosity turbulence models for engineering applications // AIAA J. 1994.Vol.32. No.8. P.1998 - 1605.
6. **Isaev S.A., Kudryavtsev, Sudakov A.G.** Numerical modeling of a turbulent incompressible viscous flow along bodies of a curvilinear shape in the presence of a mobile shield // J. Eng. Phys. and Thermophys. 1998. Vol.71. No.4. P.613-626.
7. **Isaev S.A., Guvernyuk S.V., Zubin M.A., Prigorodov Yu.S.** Numerical and physical modeling of a low-velocity air flow in a channel with a circular vortex cell // J. Eng. Phys. and Thermophys. 2000. Vol.73. No.2. P.337-344.
8. **Baranov P.A., Isaev S.A., Prigorodov Yu.S., Sudakov A.G.** Numerical analysis of the influence of the angle of attack on a turbulent flow on an incompressible fluid past a profile of large thickness with vortex cells // J. Eng. Phys. and Thermophys. 2000. Vol.73. No.4. P.705-712.
9. **Bobyshev V.K., Guvernyuk S.V., Isaev S.A.** Identification of the vortex mechanism of front stabilization in modeling of asymmetric flow of an incompressible fluid along a cylinder with a protruding disk // J. Eng. Phys. and Thermophys. 1999. Vol.72. No.4. P.606-611.
10. **Chyu M.K., Yu Y., Ding H., Downs J.P. et al.** Concavity enhanced heat transfer in an internal cooling passage // ASME Paper 97-GT-437. 1997. 7p.